Analysis of ITO on Polymer Substrate by External Bending Force

Jin-Woo Han, Young-Hwan Kim, Jong-Hwan Kim, Jeoung-Yeon Hwang, and Dae-Shik Seo[a]
Department of Electrical & Electronic Engineering, Yonsei University, Sinchon-dong, Seodaemun-gu, seoul 120-749, Korea

[a]E-mail : dsseo@yonsei.ac.kr

(Received June 17 2005, Accepted August 3 2005)

In this paper, we investigated the island density-dependent stress distribution of indium-tin-oxide (ITO) film on polycarbonate substrate by external bending force. We used e-beam and RF-sputter for SiON, ITO sputtering. It was found that there are influence of island density on the substrate and decreasing crack density as goes to the minimum density. From the result that crack density was increasing at maximum island density, it is evident that more stress is imposed on same island position as island density.

Keywords : Residual stress, Multilayer, External stress, Bending

1. INTRODUCTION

Because of being less brittle and more flexible compared to glass substrates, polymer substrate is mostly used for flexible display. Indium-tin-oxide (ITO) coatings are widely used to improve the demerits such as permeability and optical transmission of polymer substrates. Therefore, ITO coatings are used for solvent or gas resistance coatings and Transparent Conductive Oxide (TCO)[1]. Unfortunately, the brittle coatings such as ITO with large Young's modulus fail conductively when exposed to the stress above a critical limit. As a result, a crack in a conductive layer affects the resistance [2-5] and a crack in barrier coatings leads to an increased permeability. Therefore, understanding the critical stress and the failure mechanism of this coating is very important for flexible displays[6,7].

In this paper, we investigated the position-dependent stress distribution of ITO film on polycarbonate (PC) substrate by external bending force of LCD.

2. EXPERIMENTAL

We deposited six different triple-layer structures (substrate-ITO-encapsulation or substrate-buffer-ITO) com-posed of Indium-tin-oxide (ITO) and SiON or polyimide (PI) coating on polycarbonate (PC) substrate. The thickness of ITO is 200 ㎚ and the thickness of PC substrate is 180 ㎛. The process temperature was 110 °C, 120 °C for electron beam evaporated SiON and spin-coated PI curing, respectively. Young's modulus (E) and the coefficient of thermal expansion (CTE) of materials used in this experiment are defined as follows. The CTE of PC substrate or SiON and ITO is 50 ppm, 5 ppm. The Young's modulus of PC, PI or SiON, ITO is 5 GPa, 120 GPa, respectively. To investigate position dependent stress in inward bending exactly and consider flexible display device composed of pixel-arrays as ITO island-arrays, we made ITO island-arrays structure by patterned mask.

To investigate farthest cracked island position, we bent sample of 28 mm*10 mm size composed of patterned 25 and 35 ITO island-arrays to be the shape of cylindrical (L=12 mm)[5]. The farthest cracked island position is defined as island position where the farthest occurring cracks from the center position is located. From the fact that crack is fracture mechanism not elastic state, farthest cracked position and crack density are related to imposed mechanical stress in bending. Therefore, the mechanical stress such as external bending stress and residual stress can be quantified and numerically analyzed through the farthest cracked island position.

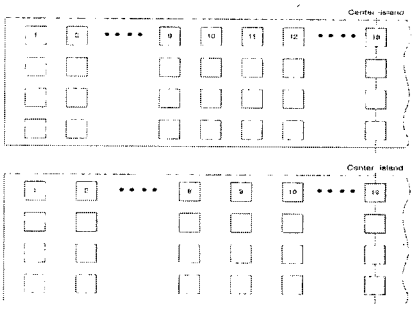

Fig. 1. Pattern consist of island arrays (25,35,45,55 islands, 520*780 ㎛^{2} in size).

3. RESULTS AND DISCUSSION

Figure 2 shows geometric shape of the substrate regarding L (face-plate distance) occurring in flexible display. The more L decreases, the more substrate change from circular shape to elliptical shape. Bending process of above Fig. 2 can be applied to PC substrate with length 28 mm used in this experiment. Figure 2(c) shows the case of the minimum L to accomplish circular shape. Therefore, if the case is that L is larger than that of hemicyclic shape as shown in Fig. 2(c), PC substrate has the arc shape (the part of circle) of the larger radius R (curvature radius) than that of hemicycle. In the case of Fig. 2(c), the length 28 mm of substrate is equal to that of hemicycle. So, introducing 28 mm=πR, R and L are calculated as R=8.91 mm, L=2R=17.8 mm, respectively. From this result, it is evident that PC substrate has the arc shape of the larger radius than R=8.91 mm of hemicycle. This means that PC substrate is bent with same curvature (R) at all position. However, in the case of L being smaller than 17.8 mm, it is evident that R of the center is gradually decreasing as L decreases. The more position is far from the center, R is more increased compared to that of the center.

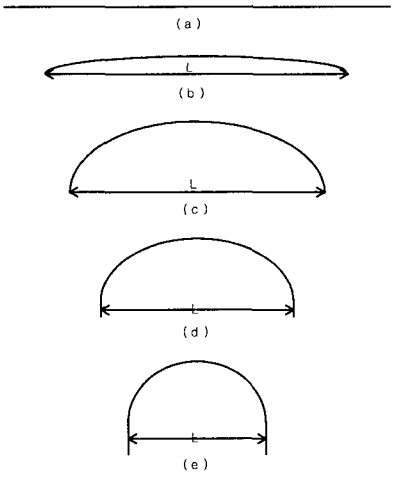

Fig. 2. Bending process.

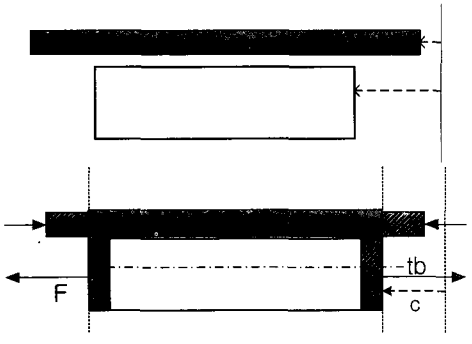

Fig. 3. The geometry of a bend.

Above discussed bending process can be explained through analysis of the bend geometry that Gulati and Matthewson presented for optical fiber shown in Curvature radius R at any point along the bend can be given by

$$2\pi R \cdot \frac{d\theta}{2\pi} = ds \tag{1}$$

$$\frac{1}{R} = \frac{d\theta}{ds} \tag{2}$$

where θ (radian) is the angle between x axis and tangent at any point and s is running along the fiber axis (in here, neutral line).

From analysis of the moment (bending force) and the bending beam equation and introducing the boundary conditions 1/R=0 at the point of force application, the following equations can be derived as

$$\frac{d\theta}{ds} = \sqrt{\frac{2F\sin\theta}{EI}} = \frac{1}{R(\theta)} \tag{3}$$

$$\frac{L}{2} = 0.847\sqrt{\frac{EI}{F}} \tag{4}$$

$$\ell = 1.854\sqrt{\frac{EI}{F}} \tag{5}$$

$$F = \frac{b \cdot h^3 \cdot C_b{}^2 \cdot E}{6L^2} \propto \frac{1}{L^2} \tag{6}$$

in which F is the force [N], E is Young's modulus [Pa], Cb is geometrical constant (=1.1985), h is sample thickness (200 ㎛), I is the moment of inertia[m^4], ℓ is half of the length of the total bend, b is sample width (10 mm).

The stress on any point at distance r from the neutral line at which the net force and stress equals zero is given by (we can assume that neutral line is located in midsurface of the PC substrate, neglecting deposited ITO film's thickness)

$$\sigma = E \cdot \frac{r}{R} \tag{7}$$

From eq. (7), the case of Fig. 2(a)~(c) indicate that same stresses are imposed on all position due to constant R regardless of position(θ). However, in the case of Fig. 2(d)~(e) , position-dependent stresses of the ITO islands is given by

$$\sigma(\theta) = r\sqrt{\frac{2EF\sin\theta}{I}} = E\cdot\frac{r}{R(\theta)} \tag{8}$$

From the fact that θ equals to π/2 in the center and θ equals to π in edge (satisfies condition 1/R=0) at fixed L (fixed F), it is evident that the stress of the center (θ=π/2) is maximum and that of the edge (θ=π) is minimum because stress is proportional to $(\sin\theta)^{1/2}$. Therefore, the stress is proportionally decreased to $(\sin\theta)^{1/2}$ as goes to the edge. The important fact is that the farthest bended position (1/R=0, θ=π) is nearer toward the center position regarding decreased L. Therefore, half of total bend length ℓ decreases proportionally regarding decreased L. This phenomenon can be understood from the bend geometry shown in Fig. 3. Combining eq. (4) and eq. (5), the proportional expression between L and ℓ can be derived as

$$\ell = \frac{L\cdot 1.854}{2\cdot 0.847} \tag{9}$$

The maximum stress σ_{max} can be derived by inserting θ=π/2 and eq. (4) into eq. (8):

$$\sigma_{max} = \frac{C_b\cdot E\cdot h}{L} = E\cdot\frac{r}{R_{min}} \tag{10}$$

Consequently, combining eq. (6) and eq. (8), the following expression can be derived as

$$\sigma(\theta) \propto \frac{\sqrt{\sin\theta}}{L} \tag{11}$$

The stress distribution corresponding to θ, d (distance from the center) regarding L

Figure 4(a) shows the stress distribution corresponding to θ (π/2≤θ≤π, 1.57≤θ≤3.14 (radian)) regarding L=10, 12, 14 mm, respectively. The resultant ℓ is calculated as 10.9445, 13.1334, 15.3223 from eq. (10), respectively. Numerical relationship between θ and distance (d) far from the center can be considered as satisfy.

$$d = \left(\frac{\ell}{\pi/2}\theta - \ell\right) = \left(\frac{L\cdot 1.854}{\frac{2\cdot 0.847}{1.57}}\cdot\theta - \frac{L\cdot 1.854}{2\cdot 0.847}\right)$$
$$= 0.6971\cdot L\cdot\theta - 1.0944L \tag{12}$$

where $\pi/2 \le \theta \le \pi$, $0 \le d \le \ell$ and $d(\theta=\pi/2)=0, d(\theta=\pi)=\ell$

Now, it is available to substitute the stress distribution dependent on θ shown in eq. (11) into the stress distribution dependent on d as follows.

$$\sigma(d) \propto \frac{\sqrt{\sin\theta}}{L} = \frac{\sqrt{\sin\left(\frac{d+1.0944L}{0.6971L}\right)}}{L} \tag{13}$$

Figure 4(b) shows the stress distribution regarding distance (d (mm)). A marked a, b, c indicate calculated distance from the center position by using proportional expression. From Fig. 4(b), at all a, b, c island position, the largest stress is imposed on the ITO islands in case of L=10 mm. As L decreases, the stress curve of near the

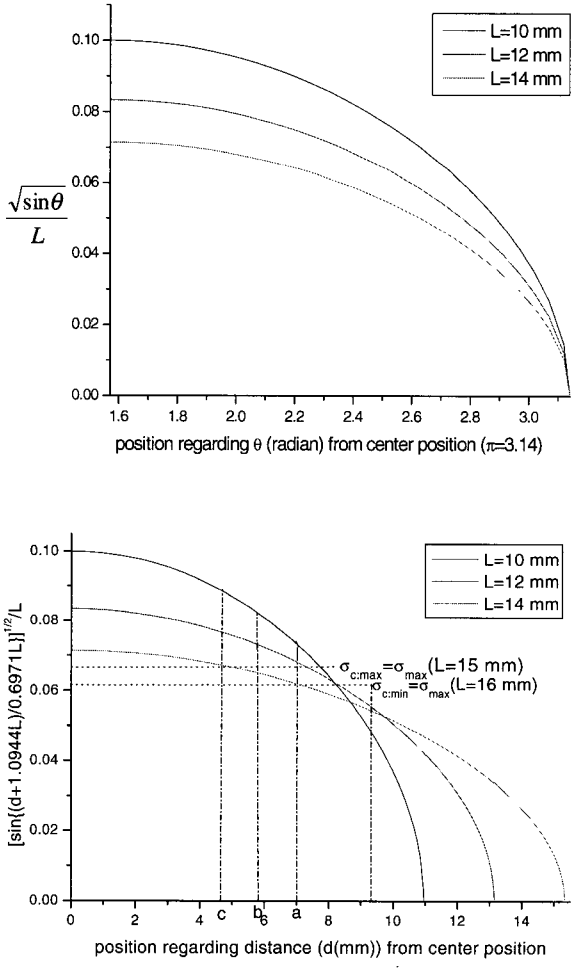

Fig. 4. Position-dependent stress distribution regarding two parameters (θ, d): (a) stress.

edge becomes gradually steeper due to decreased ℓ. As a result, though L is larger, the more stress than that of small L is imposed on ITO islands significantly far from the center. But, the critical stress σ_c can not be calculated from above derived equations. Fortunately, it can be considered from empirical results. $\sigma_{c:max}$, $\sigma_{c:min}$ shown in Fig. 4(b) is considered through the following crack investigation. On the base of above discussed theory, change of crack density and electrical resistivity was investigated to verify position-dependent stress distribution.

Figure 5 shows optical microscope images of cracking appearing in ITO islands regarding L. As shown in Fig. 5, when L =10 mm, the largest crack density is observed at 13th island position of ITO island. Because the crack density is proportional to imposed stress above critical stress, it is evident that the more stress is imposed on the center regarding decreased L due to relationship between σ ($\theta=\pi/2$) and L ; σ ($\theta=\pi/2$) $\propto$ 1/L. It is shown that the crack density of ITO island is decreased as moving from e to a island position. The farthest cracked island position of L=10, 12, 14 mm is a, b, c, respectively.

Figure 5 shows crack density at a, b, c, d, e, 13th island position regarding L. At same island position, the more crack density is observed regarding decreased L. From this result, it is evident that crack distribution between a and e island position is the same as the stress distribution shown in Fig. 4(b).

From the result of Fig. 5 the critical stress can be derived approximately. So, assuming that the critical stress is imposed on the island of the minimum crack density, $\sigma_{c:max}$ can be considered shown in Fig. 4(b). Because σ_c should be smaller than the stress of c position with L=10, 12, 14 mm. And $\sigma_{c:min}$ is considered from the fact that the cracks of L=16 mm are distributed along between 5th and 21st island position. The crack density is one or none along that region. This observance can be considered that near-uniform critical stress is imposed on along between 5th and 21st position. This observance is explained by almost same shape (uniform bending curvature near the center) alike the shape of L=18 mm. From the fact that cracks occur if only the minimum σ_{max} (L = 16 mm) is imposed on ITO island, $\sigma_{c:min}$ can be considered as shown in Fig. 4(b). Therefore, critical stress is expected to be value between σ_{max} (L = 16 mm) and σ_{max} (L = 15 mm).

Figure 7 shows the change of electrical resistivity at cracked ITO island regarding L. From Fig. 7(a) as L decreases, it is evident that the changes of electrical resistivity of ITO islands are more increased compared to that of large L. This increased electrical resistivity is explained by reduced conduction path result from increased crack density. And it is observed that the distribution of electrical resistivity change is maximum at the center and minimum at the edge like the stress distribution. Because it can not be measured at any position and only measured at given ITO islands, the distribution of electrical resistivity change can not but is discrete unlike theoretical stress distribution because of relatively large electrical resistivity change at near-center (f, 13th island) as shown in Fig. 7(b). It is evident that above phenomenon results from very narrow conduction path due significantly large stress. However, the important thing is that small L induces the larger change of electrical resistivity than large L.

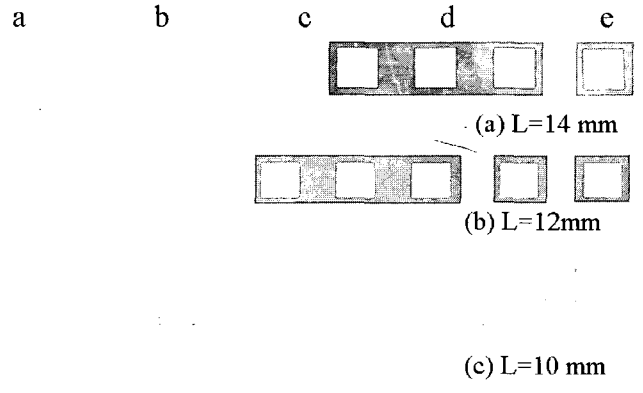

Fig. 5. Optical microscope images of cracking appearing in ITO islands regarding face-plate distance (L): (a) L=14 mm, (b) L=12 mm, and (c) L=10 mm.

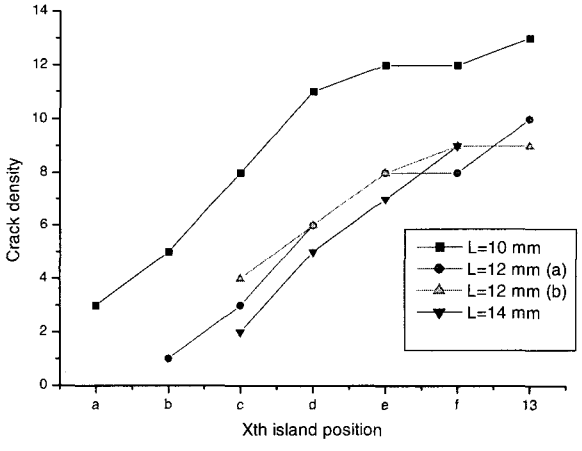

Fig. 6. Crack density at a, b, c, d, e, 13th island position regarding L.

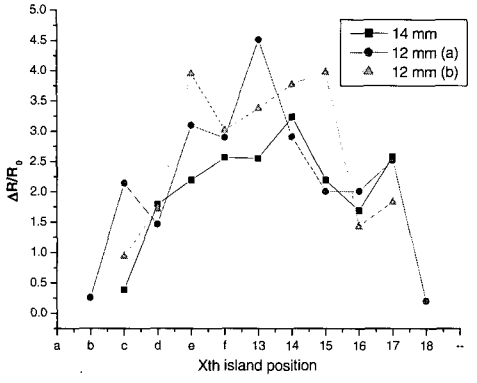

(a) at all cracked island position

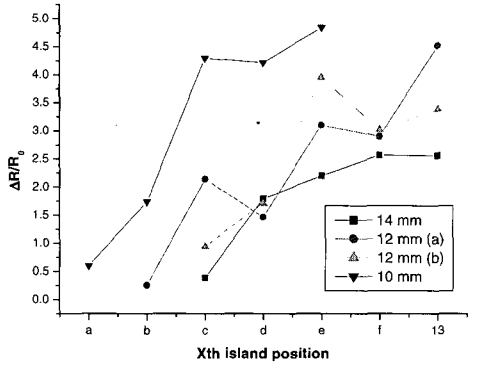

(b) at a, b, c, d, e, 13th island position

Fig. 7. The change of electrical resistivity.

Figure 8 shows that the stress distribution due to the external bending force is position-dependent and island density. Ito1, ito2, ito3, ito4 and ito5 are 25,35,45,55,60 number of island. The fact that the stress distribution is proportional to $\sqrt{\sin\theta / L}$ is proved from being the maximum crack density at the center and decreased crack density as goes to the edge. In accordance with crack distribution, this result is explained by the result that the change of electrical resistivity of the ITO islands is maximum at the center and decreases as goes to the edge.

4. CONCLUSION

In summary, encapsulation layer with small Young's modulus incorporated into devices can reduce mechanical stress on devices in external bending and less island density reduced mechanical stress. This provides the clue for improving limited flexibility in devices composed of mostly brittle oxide materials.

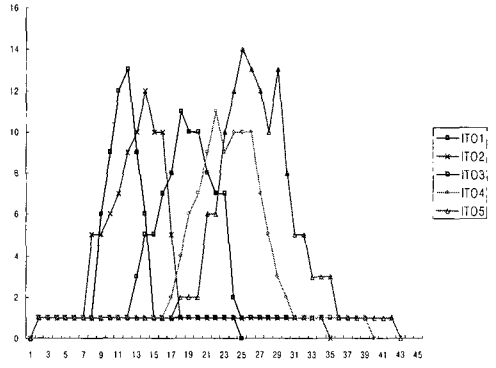

Fig. 8. The change of crack number in island density. (ito1< ito2 < ito3 < ito4 <ito5)

ACKNOWLEDGMENTS

This work was supported by National Research Laboratory program (M1-0203-00-0008).

REFERENCES

[1] D. R. Cairns, R. P. Witte II, D. K. Sparacin, S. M. Sachsman, D. C. Paine, G. P. Crawford, and R. R. Newton, "Strain-dependent electrical resistance of tin-doped indium oxide on polymer substrate", Appl. Phys. Lett., Vol. 76, No. 11, p. 1425, 2000.

[2] M. Yanaka, Y. Tsukahara, T. Okabe, and N. Takeda, "Statistical analysis of multiple cracking phenomenon of a SiO_x thin film on a polymer substrate", J. Appl. Phys., Vol. 90, No. 2, p. 713, 2001.

[3] H.-H. Kim, M.-J. Cho, W.-J. Choi, J.-G. Lee, and K. J. Lim, "Figure of merit for deposition conditions in ITO Films" , Trans. EEM, Vol. 3. No. 2, p. 6, 2002.

[4] Z. Suo, E. Y. Ma, H. Gleskova, and S. Wagner, "Mechanics of rollable and foldable film-on-foil electronics", Appl. Phys. Lett., Vol. 74, No. 8, p. 1177, 1999.

[5] S.-K. Park, J.-I. Han, D.-G. Moon, and W.-K. Kim, "Improvement of mechanical property of indium-tin-oxide films on polymer substrates by using organic buffer layer", Trans. EEM, Vol. 3. No. 2, p. 32, 2002.

[6] J.-B. Park, J.-Y. Hwang, D.-S. Seo, S.-K. Park, D.-G. Moon, and J.-I. Han, "Position dependent stress distribution of indium-tin-oxide on polymer substrate by external bending force", Jpn. J. Appl. Phys., Vol. 43, No, 5A, p. 2677, 2004.

[7] C. H. Hsueh, "Modeling of elastic deformation of multilayer due to residual stresses and external bending", J. Appl. Phys., Vol. 91, No. 12, p. 9652, 2002.